Design of a Composite Ethidium – Netropsin – Anilinoacridine Molecule for DNA Recognition

Carolina Carrasco,[a] Philippe Helissey,[b] Michelyne Haroun,[b] Brigitte Baldeyrou,[a] Amélie Lansiaux,[a] Pierre Colson,[c] Claude Houssier,[c] Sylviane Giorgi-Renault,*[b] and Christian Bailly*[a]

*Control of gene expression is a cherished goal of cancer chemotherapy. Small ligand molecules able to bind tightly to DNA in a well-defined configuration are being actively searched for. With this goal in mind, we have designed and synthesized the trifunctional molecule **R-132**, which combines a bispyrrole skeleton for minor groove DNA recognition and two different chromophores, anilinoacridine and ethidium. The affinity and mode of binding of **R-132** to DNA were studied by a combination of complementary biochemical and biophysical techniques, which included absorption and fluorescence spectroscopy and circular and linear dichroism. A surface plasmon resonance biosensor analysis was also performed to quantify the kinetic parameters of the drug – DNA interaction process. Altogether, the results demonstrate that the three moieties of the hybrid molecule are engaged in the interaction process, thus validating the rational design strategy. At the biological level, **R-132** stabilizes topoisomerase-II – DNA covalent complexes and displays potent cytotoxic activities, which are attributable to its DNA-binding properties. **R-132** easily enters and accumulates in cell nuclei, as evidenced by confocal microscopy. **R-132** therefore provides a novel lead compound for the design of gene-targeted anticancer agents.*

KEYWORDS:

antitumor agents · cytotoxicity · DNA recognition · drug design · enzymes

Introduction

Small molecules that recognize specific DNA sequences may be of great value to the rational development of novel antitumor agents.[1, 2] The ultimate goal is to design drugs able to control gene expression in cancer cells. To this end, a complete understanding of the molecular rules that govern drug – DNA sequence recognition is essential. Over the past decades, different chemical strategies have been elaborated to design molecules endowed with a high affinity for DNA and a sharp sequence selectivity. One approach that we pioneered twelve years ago consisted of covalently attaching a DNA intercalating agent to a DNA minor-groove binder to combine DNA affinity and sequence recognition.[3, 4] Several series of hybrid molecules called combilexins have been synthesized and their DNA-binding/reading properties investigated.[5, 6] The different series of combilexins reported to date by us and others contain either a planar chromophore (acridine, ellipticine, porphyrin) for intercalation between two consecutive base pairs of DNA or a photosensitizer (anthraquinone, isoalloxazine, phenazine-di-*N*-oxide) for DNA breaks, coupled to a crescent-shaped minor-groove binder. In most cases, the minor-groove binder is a polyamide heterocyclic structure related to the antibiotics netropsin and distamycin; less frequently, a peptide or an unfused aromatic system is used.[7–26] In general, these hybrid molecules have a more or less pronounced selectivity for AT-rich DNA sequences and their affinity for DNA is only slightly superior to that of the individual partners.

Some molecules in the combilexin series also revealed potent cytotoxic activities and in a few cases an in vivo anticancer effect was observed. This was the case with the combilexin molecule **NetGA**, which comprises a bispyrrole unit (an analogue of netropsin) linked through a glycine residue to an anilinoacridine moiety (an analogue of the antitumor drug amsacrine; Scheme 1). The pharmacology of this molecule was investigated in detail. We have previously shown that, 1) both the netropsin and acridine moieties play a role in the interaction with DNA,[3, 27] 2) the drug easily enters into the nucleus of cancer cells,[28] and 3) the molecule inhibits topoisomerase II to stimulate DNA

[a] *Dr. C. Bailly, Dr. C. Carrasco, B. Baldeyrou, Dr. A. Lansiaux*
INSERM U-524 et Laboratoire
de Pharmacologie Antitumorale du Centre Oscar Lambret
IRCL, Place de Verdun, 59045 Lille (France)
Fax: (+33) 320-16-92-29
E-mail: bailly@lille.inserm.fr

[b] *Prof. S. Giorgi-Renault, Dr. P. Helissey, Dr. M. Haroun*
Laboratoire de Chimie Thérapeutique
UMR 8638 CNRS, Université René Descartes (Paris 5)
Faculté des Sciences Pharmaceutiques et Biologiques
4 avenue de l'Observatoire
75270 Paris cedex 06 (France)
E-mail: S.Giorgi-Renault@pharmacie.univ-paris5.fr

[c] *Prof. P. Colson, Prof. C. Houssier*
Biospectroscopy Laboratory
Department of Chemistry, University of Liege
Sart-Tilman, 4000 Liege (Belgium)

  1439-4227/03/04/01 $ 20.00+.50/0 ChemBioChem **2003**, 4, 50 – 61

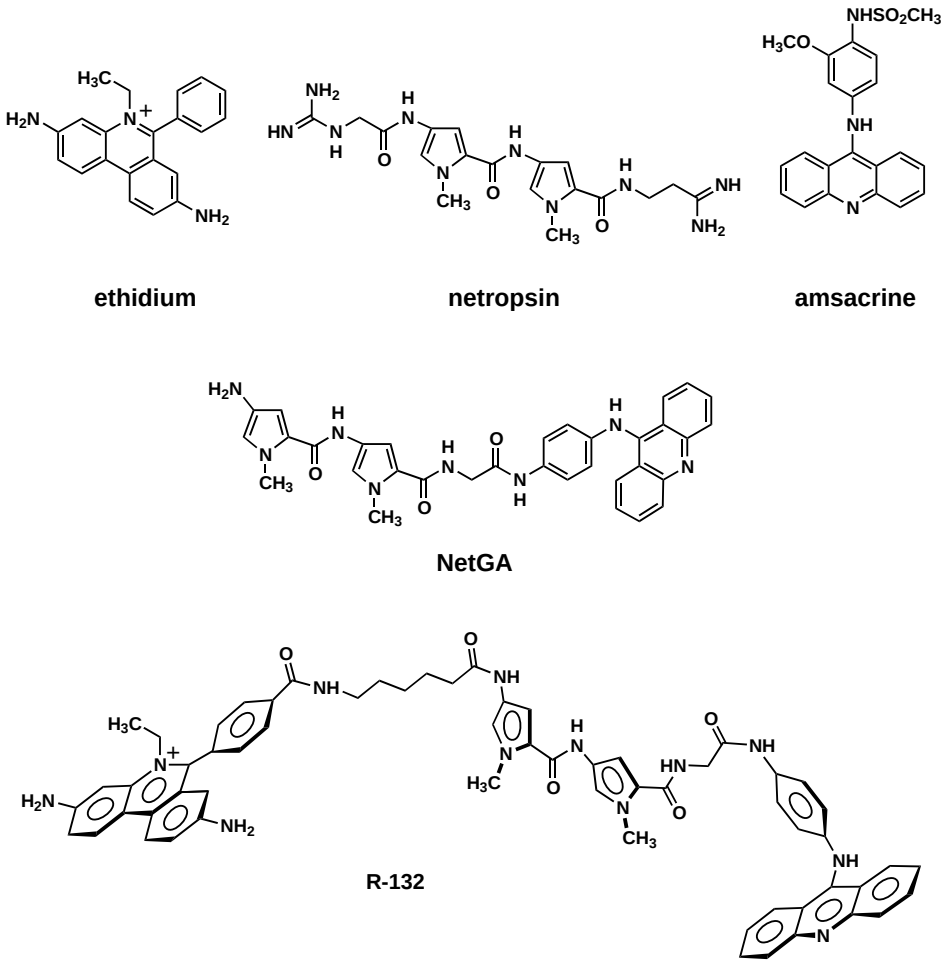

Scheme 1. *Structures of amsacrine, ethidium, netropsin,* ***NetGA*** *and* ***R-132****.*

cleavage and has antitumor activity against P388 leukaemia in mice.[8] Despite these interesting biological activities, the drug only has a relatively weak affinity for DNA, roughly equal to that of the unsubstituted acridine moiety. In an extension of this work and to reorient the chemical strategy towards drug-forming stable drug – DNA complexes, we have now covalently attached a phenylphenanthridinium chromophore to the terminal aminopyrrole ring of **NetGA**. The resulting tripartite hybrid molecule (**R-132** in Scheme 1) bears two different chromophores, anilinoacridine and ethidium, connected through a bispyrrole skeleton for minor-groove DNA recognition. To our knowledge, this is the first example of a rationally designed DNA-targeted combilexin equipped with three different well-defined functionalities. Here we report the design and synthesis of this combilexin and biochemical, biophysical, and biological studies aimed at characterizing the drug – DNA interaction and the cytotoxic properties of the new molecule **R-132**.

Results

Chemistry

In the design of the tripartite hybrid **R-132**, we decided to link the terminal aminopyrrole of **NetGA** to the phenanthridinium moiety by a polymethylenic chain in order to allow the intercalation of the second chromophore. A pentamethylenic chain was chosen by reference to a previously described monohybrid.[26] In the case of ethidium, the intercalation model suggests that the pendant phenyl ring lies in the DNA minor groove.[29] Consequently, the linker was introduced through a peptide bound to this phenyl moiety (Scheme 1). The hybrid **R-132** was obtained by a three-step convergent synthesis starting from 4-(9-acridinylamino)-*N*-glycylaniline (**5**), the oligopyrrolecarboxamide **16**, and the 3,8-diamino-6-(4-carboxyphenyl)-5-ethylphenanthridinium salt **10**; these key derivatives were prepared independently by multistep syntheses outlined in Schemes 2 – 4. The acridinyl derivative **5** was synthesized according to the method described by Hénichart[30] with some modifications (Scheme 2). We preferred to prepare compound **2** by acylation of the commercially available glycine-4-nitroaniline (**1**) instead of by acylation of *p*-nitroaniline by Boc-glycine. After catalytic hydrogenation of **2** over palladium on activated charcoal the resulting amine **3** was condensed with the 9-chloroacridine (**4**) in the presence of phenol. We used 20 equivalents of a 10-% solution of concentrated HCl in acetone for the workup instead of 10 equivalents;[30] this allowed the isolation of the dihydrochloride **5** in one step by simultaneous deprotection of the primary amino groups. In this way, derivative **5** was obtained in three steps with an overall yield of 56 %.

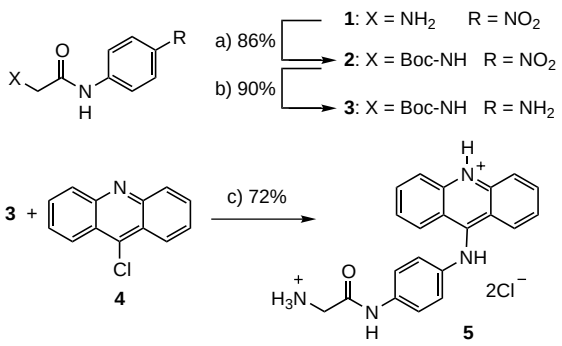

Scheme 2. *Synthesis of 4-(9-acridinylamino)-*N*-glycylaniline. a) $(Boc)_2O$, DMF, Et_3N; b) H_2, Pd/C, MeOH; c) C_6H_5OH, 70 – 80 °C, then HCl, acetone, 40 °C. Boc =* tert*-butyloxycarbonyl; DMF = dimethylformamide.*

Two synthetic pathways have been described for the synthesis of the 3,8-diamino-6-(4-carboxyphenyl)-5-methylphenanthridinium salts. The *N*-methyl analogue of **10** was described for the first time by Dervan,[31, 32] but without any experimental detail. Letsinger[33] (16% yield) and Konakahara[34] (29% yield) later published methods starting from 6-(4-cyanophenyl)-3,8-dinitrophenanthridine (**6**) that afforded the final *N*-methyl derivative in three or four steps: quaternization, partial or total hydrolysis of the nitrile groups, and chemical reduction of the nitro functions (iron-hydrochloric acid was used). In the same patent by Dervan,[32] the *N*-ethyl derivative **10** was mentioned but again without any details. With the aim of avoiding chemical reduction and subsequent difficult purification, we decided to reduce the nitro groups of **6** before quaternization (Scheme 3). Consequently, it was possible to use catalytic hydrogenation to obtain **7** and then protect the amino groups. The resulting carbamate **8** was reacted with diethyl sulfate to afford **9** in 68% yield. Removal of the protecting groups was achieved by acidic treatment and nitrile hydrolysis to give the required zwitterionic compound **10**. Thus, **10** was obtained in four steps without purification of the uncharged intermediates.

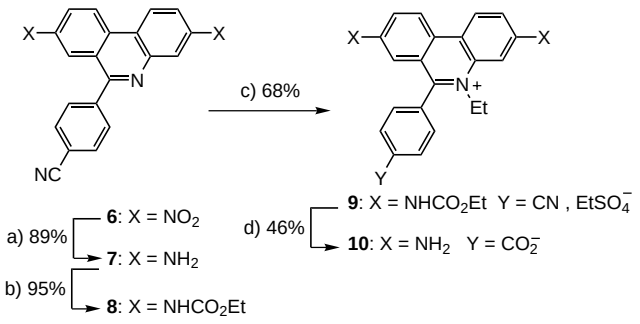

Scheme 3. *Synthesis of 3,8-diamino-6-(4-carboxyphenyl)-5-ethylphenanthridinium. a) H_2, Pd/C, MeOH; b) $ClCO_2Et$, pyridine, 15 °C; c) Et_2SO_4, DMF, 130 °C; d) H_2SO_4, 130 °C.*

The pentamethylenic carboxamido linker between the oligopyrrolecarboxamide and the phenanthridine moieties was introduced into the oligopyrrole before condensation with the two chromophores. The fully protected amino oligopyrrolecarboxamide ester **15** was obtained by peptide condensation of the amino ester **12** and 6-*tert*-butyloxycarbonylaminohexanoic acid (**14**), which were respectively synthesized by reduction of the nitro derivative **11**[35] and acylation of the commercially available 6-aminohexanoic acid (**13**). Saponification of the ester **15** afforded the acid **16** (Scheme 4).

The final sequence of the synthesis entailed formation of an amide linkage between the primary amino group of **5** and the carboxylic function of **16** (Scheme 5), quantitative removal of the Boc group by reaction with trifluoroacetic acid (TFA) on the resulting **17**, and a final peptide coupling between **18** and the acidic function of the phenanthridinium moiety **10** in the presence of EDC, HOBt, and Et_3N to give, after treatment with chlorhydric acid, **R-132** in reasonable yield.

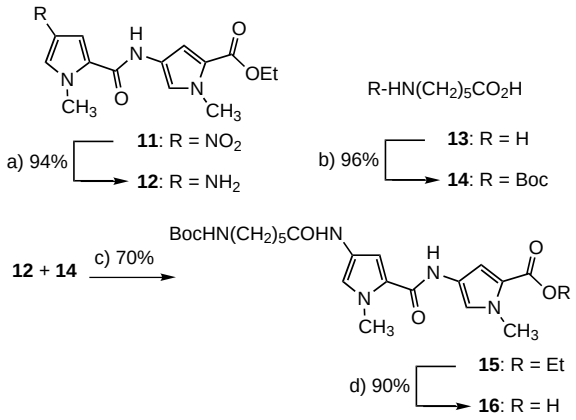

Scheme 4. *Synthesis of the oligopyrrolecarboxamide moiety. a) H_2, Pd/C, MeOH; b) $(Boc)_2O$, dioxane, H_2O, NaOH, then HCl; c) 1-(3-dimethylaminopropyl)-3-ethylcarbodiimide hydrochloride (EDC), DMF; d) NaOH, EtOH, H_2O, reflux, then HCl.*

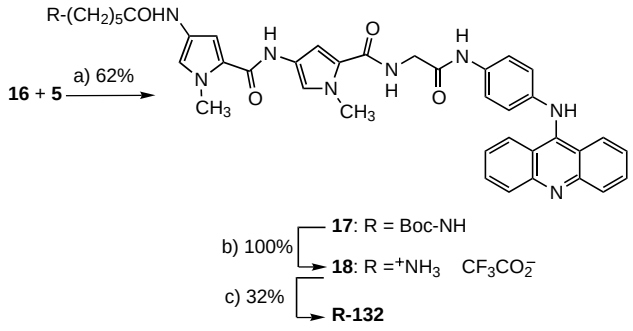

Scheme 5. *Condensation of the three moieties to give the hybrid compound **R-132**. a) EDC, 1-hydroxybenzotriazole (HOBt), Et_3N, DMF; b) TFA, 0 °C; c) **10**, EDC, HOBt, Et_3N, DMF, RT, then HCl.*

DNA affinity

Figure 1 shows the absorption spectra of **R-132** in the absence and presence of calf thymus DNA. The specific absorption bands of the three moieties of the hybrid compound can be easily

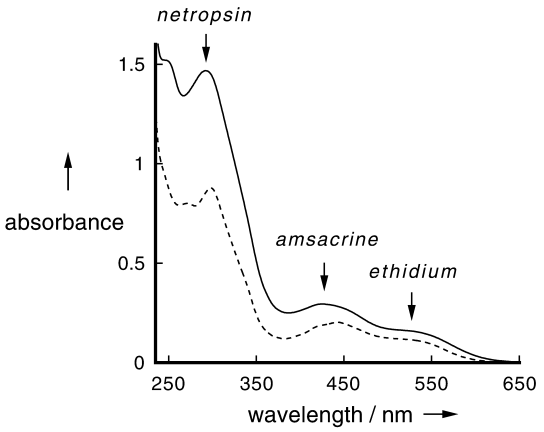

Figure 1. *Absorption spectra of a 20-μM solution of **R-132** (solid line) in the absence and (dashed line) in the presence of calf thymus DNA at a DNA-phosphate/drug (P/D) ratio of 20. The absorption measurements were performed in BPE (6 mM Na_2HPO_4, 2 mM NaH_2PO_4, 1 mM EDTA) buffer at pH 7.0.*

distinguished. The band centred at 310 nm corresponds essentially to the netropsin moiety, whereas the two chromophores anilinoacridine and ethidium absorb at higher wavelengths around 430 and 530 nm, respectively. These spectral properties will be very useful for investigation of the specific contribution of each moiety of the hybrid to interaction with DNA. Upon binding to DNA, a significant hypochromism is observed in the three bands, which suggests that the all three moieties of the hybrid ligand participate in the interaction.

To estimate the relative affinity of the hybrid compared to its individual constituents, a melting temperature (T_m) study was performed with calf thymus DNA and the polynucleotide poly(dAT)$_2$. The results of the T_m measurements on the synthetic polymer (which gives higher T_m values than the natural DNA) carried out in BPE buffer (16 mM Na^+ ions) at different drug/DNA-phosphate (D/P) ratios are presented in Figure 2. It can very clearly be seen that the hybrid ligand stabilizes duplex DNA against heat denaturation much more strongly than netropsin, amsacrine, or ethidium. For example, at a D/P ratio of 0.05, **R-132** gave a T_m value ($T_m = T_m^{complex} - T_m^{DNA}$) of 23 °C, whereas the T_m values with the three reference compounds did not exceed 3 °C. This was the first indication that the hybrid molecule binds much more tightly to DNA than its individual components.

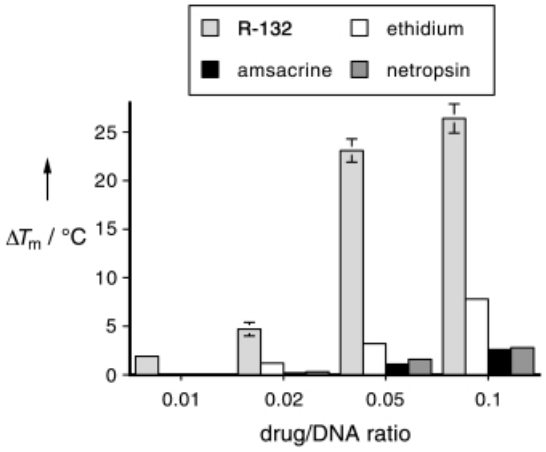

Figure 2. *Variation of the melting temperatures ΔT_m ($T_m^{drug-DNA\ complex} - T_m^{DNA\ alone}$ in °C) of the complexes between poly(dAT)$_2$ and the hybrid compound **R-132** or its individual components ethidium, netropsin, and amsacrine. The T_m measurements were performed at four P/D ratios: 0.01, 0.02, 0.05, and 0.1. The DNA concentration was fixed at 20 μM (T_m for DNA alone = 42 °C) while the drug concentration varied from 0.2 to 2 μM. T_m measurements were performed in BPE buffer (6 mM Na_2HPO_4, 2 mM NaH_2PO_4, 1 mM EDTA; pH 7.0) in 1-cm quartz cuvettes at 260 nm with a heating rate of 1 °C min^{-1}.*

We then tried to estimate the binding constant for interaction of **R-132** with calf thymus DNA by means of fluorescence spectroscopy and by taking advantage of the ethidium moiety whose fluorescence is significantly increased upon binding of the drug to DNA (Figure 3). The fluorescence at 610 nm corresponding to the ethidium moiety of **R-132** is indeed largely enhanced when the drug binds to DNA but the fluorescence yield is weak compared to that observed with ethidium bromide. Therefore, we were not able to measure the binding affinity by

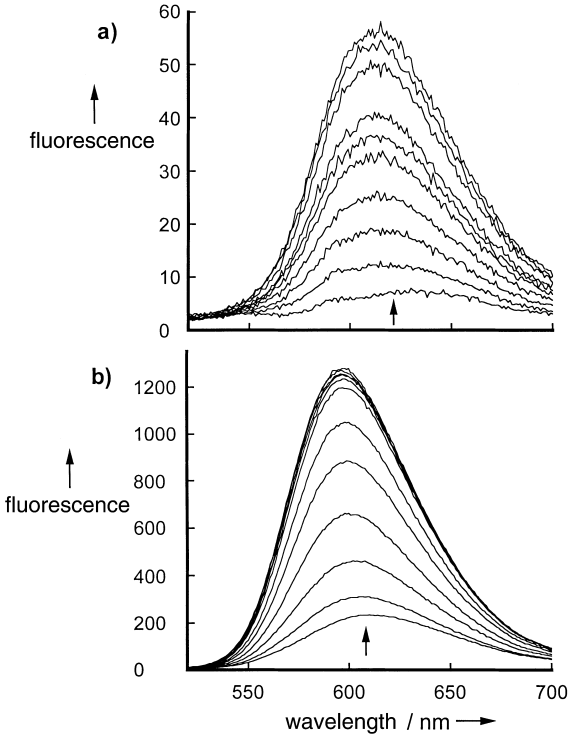

Figure 3. *Fluorescence spectra of (a) **R-132** and (b) ethidium bromide bound to calf thymus DNA. In both cases the drug concentration was maintained at 5 μM while the DNA concentration increased from 0 to 300 μM (bottom to top curves at 600 nm). Excitation wavelengths: 480 nm for **R-132** and 500 nm for ethidium, in BPE buffer at pH 7.0.*

this method. Nevertheless, this approach attested that, as expected, the ethidium moiety is involved in the interaction process, even though its orientation in the complex may well be different from that of ethidium bromide. The extent of stacking between the base pairs and the phenanthridinium ring may be distinct.

Surface plasmon resonance (SPR) experiments were conducted with a streptavidin-coated sensor chip to quantify the interaction of **R-132** with DNA. The 5′-biotin-labelled hairpin oligomer used for these experiments contained the duplex sequence d(CGAATTCG)$_2$, which should provide a good substrate for the hybrid in which the netropsin moiety interacts with the central AT pairs, and the two flanking chromophores insert near the terminal GC pairs. The oligonucleotide was immobilized on the sensor surface through streptavidin – biotin coupling and a blank flow cell was used as a control. To provide a signal directly proportional to the amount of bound compound, the reference response of this blank cell was subtracted from the response in the DNA channel. A set of SPR sensorgrams at different concentrations of **R-132** binding to the hairpin oligonucleotide is shown in Figure 4. Similar experiments were performed in parallel with ethidium bromide.

The hybrid compound **R-132** binds considerably more strongly to the CGAATTCG duplex than ethidium, in agreement with the T_m data reported above. The sensorgram results were fitted in the steady-state region as described in the Experimental Section and binding constants (K_{eq}) are collected in Table 1. The

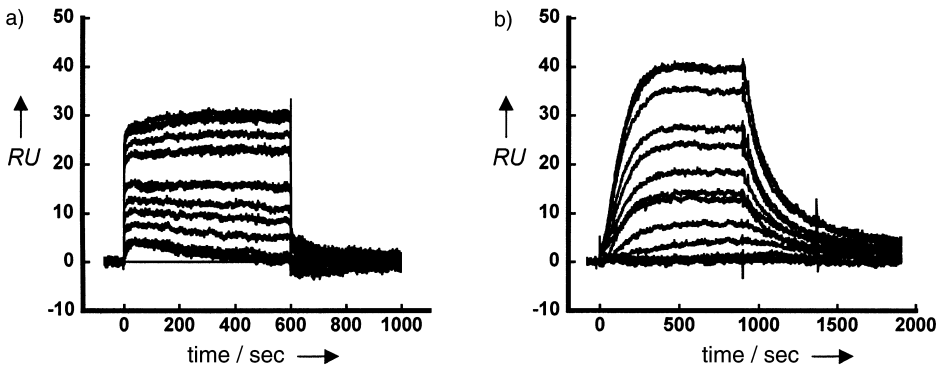

*Figure 4. SPR sensorgrams for binding of (a) ethidium bromide and (b) **R-132** to a hairpin DNA oligonucleotide containing the duplex sequence $(CGAATTCG)_2$ and a TCTC loop sequence. The unbound drug concentrations in the flow solutions range from 100 nM in the lowest curve to 1 μM in the top curve. HBS-EP buffer was used in the experiment performed at 25 °C. Fitting of the sensorgrams results in the steady-state region provided data for determination of compound binding constants, as described in the Experimental Section. These constants are collected in Table 1.*

The sensorgrams for **R-132** with the AATT sequence fit quite well with a model with one drug binding site per DNA hairpin (Langmuir 1:1, global kinetic model provided with the BIAcore software), in which the obtained residuals are very small (data not shown). It is gratifying to see that the binding constant determined by the ratio of k_a/k_d is very close to the value determined by using the more accurate steady-state fitting method (Table 1). There is no doubt that **R-132** forms stable complexes with DNA, which validates the drug design strategy.

***Table 1.** Binding and kinetic constants for ligand binding to the sequence 5′-CGAATTCG.*

	K_{eq} [M^{-1}]	k_a [MS^{-1}]	k_d [S^{-1}]	k_a/k_d [M^{-1}]
Ethidium	1.95×10^5	–[a]	–[a]	
R-132	4.81×10^6	7.92×10^4	0.0216	3.7×10^6

[a] Association (k_a) and dissociation (k_d) too fast to be measured. Experiments were performed in HBS-EP buffer.

Mode of binding to DNA

Two spectroscopic methods with polarized light were applied to define more precisely the binding process for **R-132**. Circular dichroism (CD) measurements showed that a positive band at 310 nm and negative band centred at 450 nm appeared upon addition of calf thymus DNA (Figure 5). These two CD bands reflect the orientation of the netropsin (positive CD) and acridine (negative CD) moieties bound to the double helix and are

binding constant for **R-132** binding to the duplex DNA is 25 times higher than that calculated for ethidium under exactly the same experimental conditions. Therefore, the SPR measurements agree with the T_m experiments and confirm that the hybrid exhibits a high affinity for DNA. The enhanced binding reflects the role of the netropsin – anilinoacridine moiety (**NetGA**), which serves to anchor the drug on the DNA helix. This is a strong indication that the different moieties of the hybrid participate in the DNA interaction.

As can be seen in Figure 4, both association and dissociation rates of ethidium to/from the DNA duplex are very fast, whereas the kinetics are considerably slower with **R-132**. The hybrid compound binds to the CGAATTCG target sequence in a concentration-dependent way and the association phase reaches a steady-state plateau in about 400 s (7 min), whereas it takes only a few seconds to reach the equilibrium with ethidium. The same observation can be made for the dissociation. **R-132** – oligonucleotide complexes dissociate slowly, whereas the dissociation of ethidium from the duplex is instantly obtained just by injecting buffer solution. Consequently, the kinetic parameters could not be measured for ethidium but we were able to calculate precisely the association (k_a) and dissociation (k_d) constants for **R-132** (Table 1).

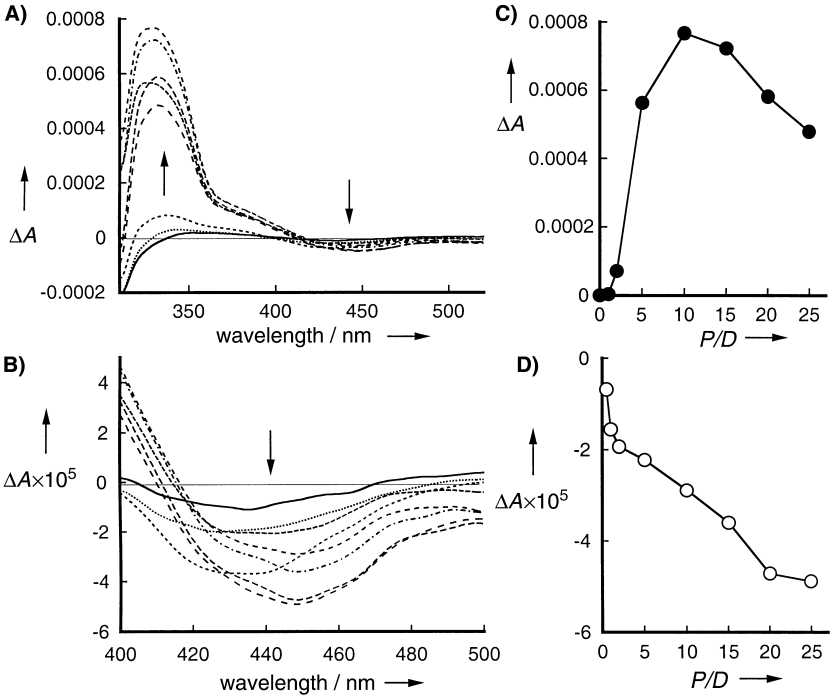

*Figure 5. CD spectra of **R-132** bound to calf thymus DNA. Panel A shows the full spectra from 310 – 500 nm, whereas panel B shows only a portion of the spectra from 400 – 500 nm. The variations of the CD amplitudes (ΔA) as a function of the P/D ratios are presented in panels C (310 nm) and D (450 nm). The solutions (3 mL) of drug bound to calf thymus DNA in sodium cacodylate buffer (1 mM, pH 7.0) were scanned in a 2-cm-pathlength quartz cuvette.*

consistent with their orientation in the minor groove and between the base pairs, respectively. No CD signal was observed in the ethidium absorption band at 530 nm.

Electric linear dichroism (ELD) measurements are very useful to estimate the orientation of the compound with respect to the DNA helix. In these experiments, the DNA is oriented by an electric field and the respective orientation of the molecules bound to DNA is probed with linearly polarized light. The ELD spectra of **R-132** bound to calf thymus DNA and the polynucleotides poly(dAT)$_2$ and poly(dGC)$_2$ are shown in Figure 6, and the dependence of the reduced dichroism $\Delta A/A$ as a function of the electric field strength is shown in Figure 7. With all three types of nucleic acids,

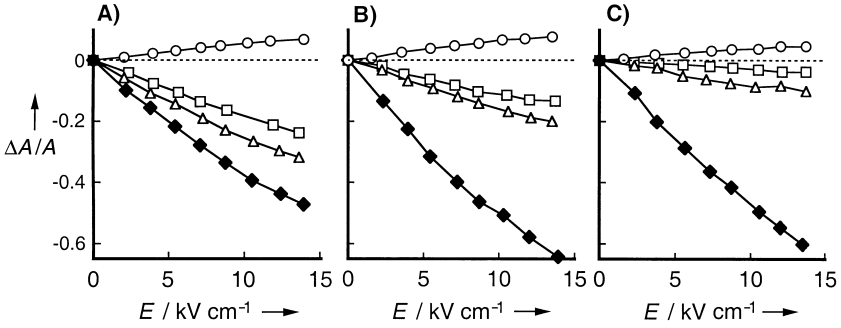

Figure 7. *Dependence of the reduced dichroism ΔA/A on the electric field strength for **R-132** bound (A) to calf thymus DNA, (B) to poly(dAT)$_2$, or (C) to poly(dGC)$_2$. The ELD measurements were performed either with (◆) DNA alone at 260 nm or with the drug–DNA complex at (○) 310 nm, (△) 440 nm, and (□) 530 nm. P/D = 20 (200 μM DNA, 10 μM drug), in 1 mM sodium cacodylate buffer at pH 7.0.*

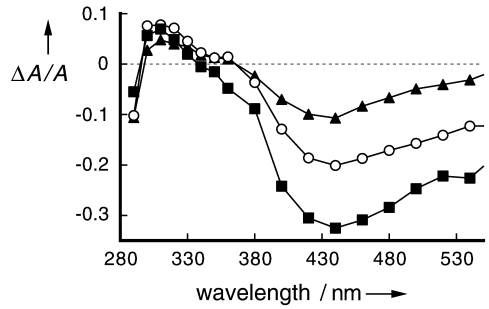

Figure 6. *Reduced ELD (ΔA/A) spectra of **R-132** bound to (■) calf thymus DNA, (○) polyd(A-T)$_2$, or (▲) polyd(G-C)$_2$. ELD data were recorded in the presence of 200 μM polynucleotide and 10 μM drug, in 1 mM sodium cacodylate buffer at pH 7.0 under a field strength of 14 kV cm^{-1}.*

the reduced dichroism $\Delta A/A$ is negative in the 440 and 530 nm bands corresponding to the anilinoacridine and ethidium absorption bands, respectively. In contrast, the reduced dichroism is positive in the netropsin absorption band at 310 nm. The positive or negative ELD signals are weaker with poly(dGC)$_2$ than with poly(dAT)$_2$, which suggests that the latter polymer is preferred over the former; however, stable complexes were obtained in both cases. With calf thymus DNA, which can provide a large variety of binding sites with all sorts of AT/GC base pair (bp) combinations, the reduced dichroism values measured at 440 and 530 nm are not as negative as those measured for DNA alone at 260 nm. At first sight, this observation suggests that the two acridine and phenanthridine chromophores are not oriented parallel to the DNA base pairs. Alternatively, it is possible that the two chromophores are fully intercalated between the base pairs but that the DNA helix axis is locally bent at the drug binding sites. The exact structure of the **R-132**–DNA complex cannot be fully determined by this spectroscopic method; however, these ELD data are entirely consistent with the T_m, fluorescence, SPR, and CD data, which all suggest that the three moieties of the hybrid are engaged in the interaction with DNA.

Sequence preference

A ^{32}P-labeled DNA restriction fragment of 176 base pairs was used as a substrate for the DNase I footprinting experiments. A sequencing gel used to fractionate the products of partial digestion of the DNA fragment complexed with **R-132** is shown in Figure 8. At concentrations below 1 μM there was practically no inhibition of DNase I cutting, whereas at 2.5 μM the hybrid molecule strongly affected the cleavage of the DNA substrate by the nuclease. At 5 μM no more DNA cutting was observed,

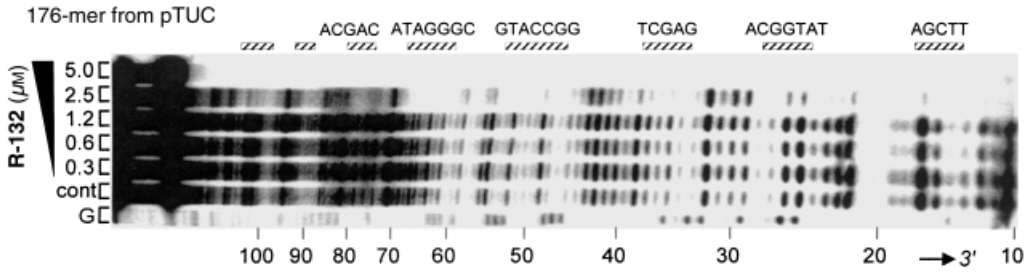

Figure 8. *DNase I footprinting gel obtained with a radiolabeled 176-bp DNA restriction fragment in the presence of graded concentrations of **R-132**. The DNA was 3′-end labeled with [α-^{32}P]dATP (ATP = adenosine triphosphate) in the presence of AMV reverse transcriptase. The drug concentrations vary from 0.3 to 5.0 μM. The products of nuclease digestion were resolved on an 8% polyacrylamide gel containing 7 M urea. The control track (cont) contained no drug. Guanine-specific sequence markers obtained by treatment of the DNA with dimethylsulfate followed by piperidine were run in the lane marked G. Numbers at the bottom of the gel refer to the standard numbering scheme for the nucleotide sequence of the DNA fragment. Bars and sequences indicate the sites of reduced cleavage by DNase I in the presence of the drug at 2.5 μM.*

presumably as a result of the tight and nonspecific association of the drug with the DNA, but an additional direct interaction with the enzyme cannot be excluded. At 2.5 μM, the drug protects a number of short sequences (5 – 7 bp in length) from DNase I cleavage. These sequences correspond essentially to GC-rich sites, as indicated in Figure 8. Attempts to identify specific binding sites were unsuccessful. The drug can obviously interact with a large variety of DNA sequences without precise selectivity.

Topoisomerase II inhibition

The effect of the hybrid compound on the catalytic activity of human topoisomerases I and II was investigated by using a conventional plasmid DNA relaxation assay.[36] As shown in Figure 9A, the hybrid strongly perturbs the electrophoretic mobility of the DNA in the presence of topoisomerase I; however, it does not act as a poison for this enzyme. **R-132** does not promote single-stranded DNA cleavage by the enzyme. At concentrations of 5 – 10 μM, the amount of nicked DNA molecules remains minimal, which indicates that the drug does not stabilize topoisomerase-I – DNA covalent complexes. The observed unwinding effect is typical of an intercalating agent (Figure 9B).

The DNA relaxation assays performed with human topoisomerase II reveal that **R-132** behaves as a poison for this enzyme (Figure 9C). The stimulation of double-stranded DNA cleavage manifests itself by the appearance of a band in the gel (between the nicked and supercoiled forms) corresponding to linear DNA (Figure 9C). A similar band also appears in the presence of the hybrid although its intensity is weaker than with the antitumor drug etoposide, which is known to efficiently stabilize topoisomerase-II – DNA complexes. If we compare these results with previous data obtained with the netropsin – anilinoacridine hybrid **NetGA**,[7] it appears that the new trifunctional hybrid is equally efficient at inhibiting topoisomerase II compared to its parent compound. The capacity of the anilinoacridine derivative to inhibit topoisomerase II is preserved when the ethidium moiety is incorporated.

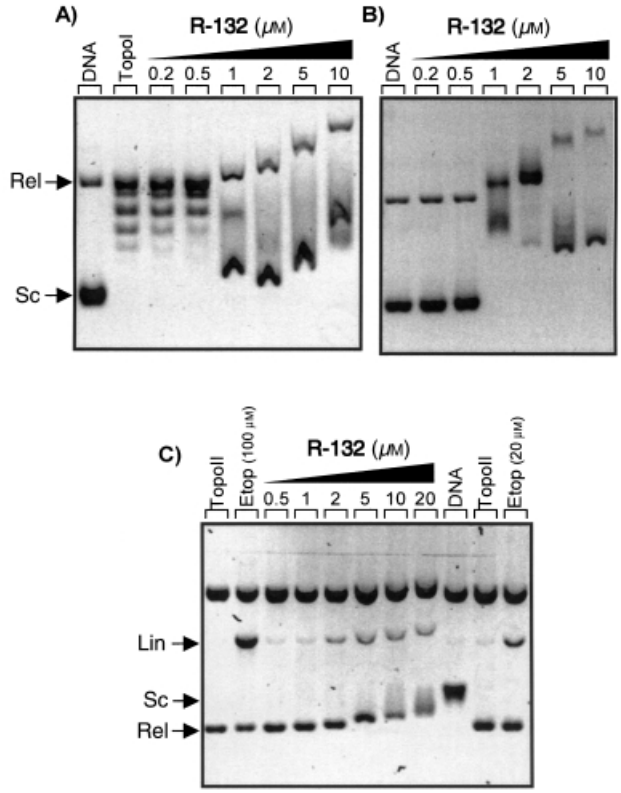

Figure 9. *Effect of increasing concentrations of compound **R-132** on the relaxation of plasmid DNA by (A) topoisomerase I and (C) topoisomerase II, or without enzyme (B). In (A), native supercoiled pKMp27 DNA (0.5 μg; lane DNA) was incubated with topoisomerase I (4 units) in the absence (lane Topol) or presence of **R-132** at the indicated concentration (μM). Reactions were stopped with sodium dodecylsulfate and treatment with proteinase K. DNA samples were separated by electrophoresis on a 1% agarose gel and then stained with ethidium bromide. In (B), the same experiment was performed without enzyme. In (C), supercoiled pKMp27 DNA (0.5 μg; lane DNA) was incubated with topoisomerase II (4 units) in the absence (lane TopoII) or presence of the drug at the indicated concentration (μM). Etoposide (Etop) was used at 20 and 100 μM, as indicated. Reactions were stopped by treatment with SDS and proteinase K. DNA samples were separated by electrophoresis on an agarose gel containing ethidium bromide (1 μg mL^{-1}). The gels were photographed under UV light. Lin, linear; Rel, relaxed; Sc, supercoiled.*

Intracellular distribution and cytotoxicity

The fluorescence of ethidium bromide and the ethidium moiety of **R-132** is significantly increased upon binding of the drugs to DNA (Figure 3). This property can be very useful to locate the drug molecules in cells providing that they can easily cross the cell membranes. It is well known that the plasma membrane strongly limits the uptake of ethidium bromide into cells and little, if any, fluorescence of DNA-bound ethidium bromide molecules can be detected in the nuclei if the cells are not permeabilized. In sharp contrast, no permeabilization is required for **R-132** to enter cells and stain nucleic acids. P388 leukemia cells were treated with **R-132** prior to the analysis of the intracellular distribution profile of the drug by means of confocal microscopy. The typical image presented in Figure 10 clearly shows that the bright red fluorescence is specifically located in the cell nuclei. These cells are thus fully permeable to **R-132**, whereas parallel experiments performed with ethidium bromide under identical conditions showed practically no intracellular

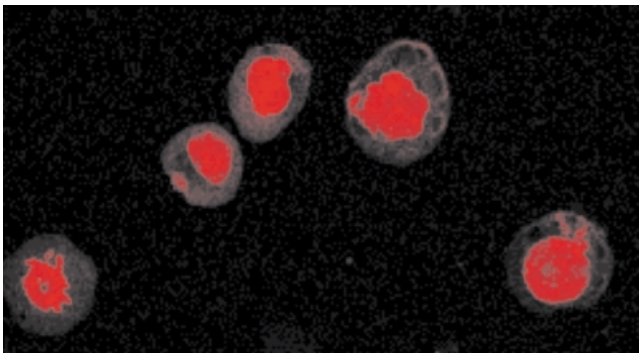

Figure 10. *Intracellular distribution of **R-132** (10 μM) in P388 murine leukemia cells visualized by confocal fluorescence microscopy (× 63) after 18 h incubation. Red fluorescence indicates localization of the drug predominantly in the nuclei.*

fluorescence, unless the cells were permeabilized with ethanol. The acridine – netropsin moiety of **R-132** is probably responsible for the enhanced uptake, since the drug **NetGA** has been shown to enter cells very easily.[28]

The cytotoxic potential of **R-132** was assessed by a conventional cell growth inhibition assay after 3 days continuous exposure to P388 mouse leukaemia cells. IC_{50} values of 0.7, 1.0, and 0.4 μM were measured with **R-132**, amsacrine, and ethidium, respectively. The cytotoxic potential of the hybrid compound is thus comparable to that of the related mono-intercalating agents.

Discussion

Over the past ten years, we have developed different series of combilexin molecules containing two distinct DNA-interacting groups for minor groove binding and intercalation in DNA.[4, 5] We initiated the design of bifunctional molecules that associate a netropsin/distamycin-like minor-groove binder with a planar chromophore such as acridine or an ellipticine derivative. We have also elaborated more complex molecules containing a DNA-threading intercalator and/or a DNA-cleaving agent.[7, 20, 26] Here, we have extended the strategy to incorporate two different intercalating agents disposed on both sides of a crescent-shaped minor-groove binder. The pentamethylenic carboxamido bispyrrole unit of compound **R-132** was selected to serve as a linker between the acridine and phenanthridine nuclei while maintaining both the isoconcavity required to optimally complement the DNA minor groove surface and the necessary flexibility for intercalation of the second chromophore. The three DNA-binding groups in **R-132** were chosen for their DNA-binding properties but also for their spectral properties. The ethidium, anilinoacridine, and netropsin moieties absorb light at different wavelengths with relatively little overlap, thus enabling an estimation of their specific interaction with DNA through the use of different spectroscopic techniques.

The combined UV, CD, ELD, and fluorescence measurements indicate that the three moieties of the hybrid ligand **R-132** are all implicated in the DNA interaction. It is not possible at the present time to determine the architecture of the drug – DNA complex with any greater detail but nevertheless the data are fully compatible with a model in which the central bispyrrole unit of the composite molecule occupies the minor groove of the double helix, with the two appended chromophores intercalated between adjacent base pairs. The T_m and SPR measurements reveal that the affinity of the hybrid for DNA is considerably higher than that of its individual components, which provides evidence that the three moieties of the hybrid are engaged simultaneously in the DNA interaction. BIAcore technology proved extremely useful to determine the kinetic parameters of the drug – DNA interaction. The fact that the complex between **R-132** and DNA dissociates much more slowly than the corresponding DNA complex with ethidium is a strong indication that all the different moieties of the hybrid are engaged in the interaction. We can safely conclude that we have succeeded in designing and synthesizing a ligand that binds tightly to DNA in a concerted intercalation and minor-groove-binding mode. However, if both the affinity and stability of the drug – DNA complex have been significantly increased, this is at the expense of sequence selectivity because the new hybrid does not appear to recognize any precise DNA sequence. In our earlier attempts at designing bifunctional molecules built on the netropsin intercalator concept, we have always observed that the AT-selectivity of the netropsin/distamycin moiety was reduced when an intercalating agent was coupled to the minor-groove-binding element, whatever the length and flexibility of the linker. Here, the additional gain of DNA affinity is accompanied by a loss of sequence selectivity. The fact that the netropsin moiety of **R-132** does not play the fully expected role of recognizing specific sequences suggests that it is probably not deeply inserted into the minor groove and thus it may not engage molecular contacts with AT base pairs.

Conclusion

The geometry of the linker has to be optimized in future drug design with this series. It may be preferable to replace the rigid bispyrrole linker with a more flexible tether that could better adapt to the conformational and dynamic characteristics of the target DNA sequences. For this reason, we are currently synthesizing new trifunctional hybrid analogues of **R-132** that incorporate peptide linkers able to direct the binding in the DNA major groove.[37]

At the biological level, the hybrid **R-132** shows interesting properties. It behaves as a conventional poison capable of stabilizing topoisomerase II enzyme – DNA covalent complexes. **R-132** produces a significant amount of topoisomerase-II-mediated double-stranded DNA breaks, as previously observed with the hybrid **NetGA**.[7] Apparently, the incorporation of the ethidium moiety has no influence on the capacity of the drug to inhibit topoisomerase II. The cytotoxicity of **R-132** can thus be attributed to at least two types of molecular action: DNA binding and topoisomerase II inhibition. Several of the most familiar drugs in the cancer chemotherapeutic arsenal (e.g. daunomycin, amsacrine, mitoxantrone) are thought to act in this way, by disorganizing the structures and functions of DNA and topoisomerase II. The preliminary biological evaluation reported here indicates that **R-132** is a potent cytotoxic agent and is encouraging for the future development of this series of combilexin molecules.

Experimental Section

Chemical synthesis:

General: Melting points were determined on a Maquenne apparatus and are uncorrected. The IR spectra were recorded on a Perkin – Elmer FTIR 1600 spectrophotometer and only the principal sharply defined peaks are reported. The NMR spectra were recorded on a Bruker AC-300 spectrophotometer (1 H, 300 MHz; ^{13}C, 75 MHz). DCI mass spectra were measured on a Nermag R10 – 10C, a quadrupole instrument, and ESI/HR spectra were acquired on a QTOF/Micromas mass spectrometer. Thin-layer chromatography was carried out on Merck GF 254 silica gel plates. Flash chromatography was performed on silica gel (Silice 60 ACC, 35 – 70 μm).

4-Nitro-*N*-(*tert*-butyloxycarbonylglycyl)aniline (2): Di-*tert*-butyldicarbonate (2.40 g, 11 mmol) and Et_3N (1.68 mL, 12 mmol) were added to a solution of 4-nitro-*N*-glycylaniline (**1**; 1.95 g, 10 mmol) in DMF (10 mL). The reaction mixture was stirred at room temperature for 12 h. After addition of water, the precipitate was filtered off, washed with water, dried, and purified by flash chromatography (dichloromethane/MeOH, 100:0 – 95:5) to give **2** as a yellow powder (2.54 g, 86%). M.p.: 210 °C (Ref. [30]: m.p.: 210 °C).

4-Amino-*N*-(*tert*-butyloxycarbonylglycyl)aniline (3): A suspension of nitro derivative **2** (1.8 g, 6.10 mmol) in MeOH (300 mL) was hydrogenated for 4 h at room temperature under a 5-bar pressure in the presence of 10% Pd on activated charcoal (1 g). The catalyst was then removed by filtration and the MeOH was evaporated under reduced pressure. The resulting residue was washed with Et_2O to give **3** as a white solid (1.46 g, 90%). M.p.: 150 °C (Ref. [30]: m.p.: 143 – 145 °C).

4-(9-Acridinylamino)-*N*-glycylaniline dihydrochloride (5): 4-Amino-*N*-(*tert*-butyloxycarbonylglycyl)aniline (**3**; 1.50 g, 5.65 mmol) was added to a solution of 9-chloroacridine (**4**; 1.2 g, 5.65 mmol) in phenol (15 mL) at 70 – 80 °C. The reaction mixture was stirred for 1 h at 75 °C and then cooled to 40 °C. After addition of concentrated HCl (10 mL) and acetone (100 mL), the stirring was continued for 1 h at room temperature. The resulting brick-red precipitate was filtered off, washed with acetone, and then purified by flash chromatography (dichloromethane/MeOH, 85:15 to 50:50) to give compound **5** (1.69 g, 72%). M.p.: 258 °C [Ref. [30]: m.p.: 258 – 260 °C (HCl and TFA salt)].

3,8-Diamino-6-(4-cyanophenyl)phenanthridine (7): A suspension of compound **6**[34] (2.22 g, 6.00 mmol) in MeOH (600 mL) was hydrogenated for 48 h at room temperature under a 5-bar pressure in the presence of 10% Pd on activated charcoal (1 g). The catalyst was then removed by filtration and the solvent was evaporated under reduced pressure to give a brown-red solid (1.66 g, 89%), which was used without further purification for the next step. IR (KBr): $\tilde{\nu} = 3410, 3311, 3225, 2224\ cm^{-1}$; ^1H NMR ([D$_6$]DMSO): $\delta = 5.60$ (4H, br s; $2NH_2$), 6.88 (1H, d, $J = 2$ Hz; H_4 or H_7), 7.05 (1H, dd, $J = 2$, $J = 9$ Hz; H_2 or H_9), 7.08 (1H, d, $J = 2$ Hz; H_4 or H_7), 7.22 (1H, dd, $J = 2$, $J = 9$ Hz; H_2 or H_9), 7.84 (2H, d, $J = 9$ Hz; $H_{2'}$, $H_{6'}$), 8.06 (2H, d, $J = 9$ Hz; $H_{3'}$, $H_{5'}$), 8.29 (1H, d, $J = 9$ Hz; H_1 or H_{10}), 8.40 (1H, $J = 9$ Hz; H_1 or H_{10}) ppm; ^{13}C NMR ([D$_6$]DMSO): $\delta = 108.2$ (CH), 110.9 (CH), 111.9 (Cq), 116.3 (Cq), 118.9 (CH), 119.8 (CN), 122.4 (CH), 123.0 (CH), 123.6 (CH), 125.1 (Cq), 125.9 (Cq), 131.4 (2CH), 133.2 (2CH), 144.2 (Cq), 145.9 (Cq), 147.6 (Cq), 148.9 (Cq), 158.2 (Cq) ppm; MS (DCI/NH_3): *m/z*: 311 $[MH]^+$.

6-(4-Cyanophenyl)-3,8-diethoxycarbonylaminophenanthridine (8): Ethyl chloroformate (0.9 mL, 9.50 mmol) was added to a solution of derivative **7** (1.5 g, 4.85 mmol) in pyridine (40 mL) at 15 °C. The reaction mixture was stirred at room temperature for 4.5 h. Addition of water gave a precipitate, which was washed with water and then purified by heating at reflux in water (500 mL) for 2.5 h. The resulting hot suspension was filtered off and the precipitate was washed with water to provide **8** as a yellow powder (2.09 g, 95%). This product was used without further purification for the next step. An analytical sample was purified by flash chromatography (dichloromethane/MeOH, 90:10). M.p.: 275 – 276 °C; IR (KBr): $\tilde{\nu} = 3334, 2232, 1714\ cm^{-1}$; ^1H NMR ([D$_6$]DMSO): $\delta = 1.24$ (3H, t; CH_2CH_3), 1.31 (3H, t; CH_2CH_3), 4.14 (2H, q; CH_2CH_3), 4.21 (2H, q; CH_2CH_3), 7.85 (1H, dd, $J = 2$, $J = 9$ Hz; H_2 or H_9), 7.92 (2H, d, $J = 9$ Hz; $H_{2'}$, $H_{6'}$), 8.00 (1H, dd, $J = 2$, $J = 9$Hz; H_2 or H_9), 8.10 (2H, d, $J = 9$ Hz; $H_{3'}$, $H_{5'}$), 8.21 (1H, d, $J = 2$ Hz; H_4 or H_7), 8.25 (1H, d, $J = 2$ Hz; H_4 or H_7), 8.67 (1H, d, $J = 9$Hz; H_1 or H_{10}), 8.77 (1H, d, $J = 9$ Hz; H_1 or H_{10}), 10.02 (1H, s; NH), 10.07 (1H, s; NH) ppm; ^{13}C NMR ([D$_6$]DMSO): $\delta = 15.5$ ($2CH_3$), 61.4 ($2OCH_2$), 112.4 (Cq), 115.3 (CH), 117.5 (CH), 119.7 (CN, Cq), 120.4 (CH), 123.8 (CH), 123.9 (CH), 124.3 (CH), 125.0 (Cq), 129.2 (Cq), 131.6 (2CH), 133.3 (2CH), 139.1 (Cq), 140.5 (Cq), 144.2 (Cq), 145.1 (Cq), 154.6 (2CO), 159.7 (Cq) ppm; elemental analysis calcd (%) for $C_{26}H_{22}N_4O_4 \cdot 1H_2O$ (472.5): C 66.09, H 5.12, N 11.86; found: C 65.66, H 5.18, N 11.79.

6-(4-Cyanophenyl)-3,8-diethoxycarbonylamino-5-ethylphenanthridinium ethyl sulfate (9): A solution of compound **8** (600 mg, 1.32 mmol) and diethyl sulfate (3 mL, 22.9 mmol) in DMF (6 mL) was heated at 130 °C for 6 h. After cooling, the precipitate was filtered off. A further amount of diethyl sulfate (1 mL, 7.64 mmol) was added to the filtrate. After 6 h of heating, a new precipitate was filtered off. The combined precipitates were washed with a mixture of dichloromethane/MeOH (50:50) and then with dichloromethane. Purification by flash chromatography (dichlomethane/MeOH, 95:5 to 90:10) yielded a yellow powder (546 mg, 68%). M.p.: 294 °C (decomp.); IR (KBr): $\tilde{\nu} = 3250, 2234, 1728\ cm^{-1}$; ^1H NMR ([D$_6$]DMSO): $\delta = 1.10$ (3H, t; CH_2CH_3), 1.20 (3H, t; CH_2CH_3), 1.30 (3H, t; CH_2CH_3), 1.50 (3H, t; CH_2CH_3), 3.80 (2H, q; $CH_3CH_2SO_4$), 4.15 (2H, q; OCH_2CH_3), 4.27 (2H, q; OCH_2CH_3), 4.62 (2H, q; NCH_2CH_3), 7.62 (1H, d, $J = 2$ Hz; H_7), 8.05 (3H, m; H_2, $H_{2'}$, $H_{6'}$), 8.35 (3H, m; H_9, $H_{3'}$, $H_{5'}$), 8.77 (1H, d, $J = 2$ Hz; H_4), 9.06 (1H, d, $J = 9$ Hz; H_{10}), 9.11 (1H, d, $J = 9$ Hz; H_1), 10.25 (1H, s; NH), 10.55 (1H, s; NH) ppm; ^{13}C NMR ([D$_6$]DMSO): $\delta = 14.8$ (CH_3), 15.4 ($2CH_3$), 16.2 (CH_3), 51.8 (NCH_2), 61.9 (OCH_2), 62.2 ($2OCH_2$), 107.4 (CH), 115.0 (Cq), 117.8 (CH), 119.2 (CN), 122.2 (Cq), 122.8 (CH), 124.7 (CH), 126.3 (Cq), 126.4 (CH), 129.7 (CH), 130.6 (2CH), 131.0 (Cq), 134.4 (2CH), 134.7 (Cq), 136.9 (Cq), 141.0 (Cq), 143.3 (Cq), 154.4 (CO), 154.7 (CO), 161.9 (Cq) ppm; elemental analysis calcd (%) for $C_{30}H_{32}N_4O_8S \cdot 1H_2O$ (626.7): C 57.49, H 5.47, N 8.94; found: C 57.44, H 5.35, N 8.93.

3,8-Diamino-6(4-carboxyphenyl)-5-ethylphenanthridinium (10): A solution of phenanthridinium salt **9** (517 mg, 0.850 mmol) in 75% sulphuric acid (8.0 mL) was heated to 130 °C for 7 h. After cooling, the reaction mixture was poured onto ice and concentrated NaOH was added until a pH value of 5 was reached. The mixture was evaporated and the resulting residue was triturated with a mixture of dichloromethane/MeOH (50:50) and then filtered off. After removal of the solvent, the residue was purified by flash chromatography (dichloromethane/MeOH, 95:5 to 90:10) to give acid **10** as a red-purple powder (140 mg, 46%). M.p.: 217 – 218 °C; IR (KBr): $\tilde{\nu} = 3308, 3194$ (broad bands), $1618\ cm^{-1}$; ^1H NMR ([D$_6$]DMSO): $\delta = 1.45$ (3H, t; CH_2CH_3), 4.48 (2H, q; CH_2CH_3), 5.90 (2H, br s; NH_2), 6.23 (1H, d, $J = 2$ Hz; H_7), 6.35 (2H, br s; NH_2), 7.35 (2H, m; H_2, H_4), 7.55 (1H, dd, $J = 2$ Hz, $J = 9$ Hz; H_9), 7.82 (2H, d, $J = 9$ Hz; $H_{2'}$, $H_{6'}$), 8.25 (2H, d, $J = 9$ Hz; $H_{3'}$, $H_{5'}$), 8.63 (1H, d, $J = 9$ Hz; H_{10}), 8.68 (1H, d, $J = 9$ Hz; H_1) ppm; ^{13}C NMR ([D$_6$]DMSO): $\delta = 14.7$ (CH_3), 50.3 (CH_2), 99.4 (CH), 108.7 (CH), 118.6 (Cq), 121.1 (CH), 123.7 (CH), 125.7 (CH), 125.8 (Cq), 128.6 (Cq), 129.0 (CH), 130.0 (2CH), 131.1 (2CH), 133.9 (Cq), 135.2 (Cq), 137.3 (Cq), 149.1 (Cq), 152.2 (Cq), 158.5 (Cq), 167.8 (CO) ppm; MS (DCI/NH_3): *m/z*: 358 $[MH]^+$.

6-*tert*-Butyloxycarbonylaminohexanoic acid (14): Di-*tert*-butyldicarbonate (13.1 g, 60 mmol) was added to a solution of 6-aminohexanoic acid **13** (6.55 g, 50 mmol) in a mixture of 2 M NaOH (75 mL), water (125 mL) and dioxane (200 mL). The reaction mixture was stirred at room temperature for 12 h, and then concentrated. After acidification with concentrated HCl, the aqueous phase was extracted with dichloromethane. The combined organic phases were washed with water, dried over Na_2SO_4, and evaporated to afford pure **14** (11.1 g, 96%). M.p.: 44 – 46 °C, IR (KBr): $\tilde{\nu} = 3384, 1711, 1687\ cm^{-1}$; ^1H NMR ($CDCl_3$): $\delta = 1.40$ (13H, m; $C(CH_3)_3$, $2CH_2$), 1.55 (2H, m; CH_2), 2.28 (2H, t; CH_2CO), 3.05 (2H, m; $NHCH_2$), 4.50 (1H, m; $NHCH_2$), 10.30 (1H, s; OH) ppm; ^{13}C NMR ($CDCl_3$): $\delta = 24.3$ (CH_2), 26.2 (CH_2), 28.4 ($3CH_3$), 29.6 (CH_2), 33.9 (CH_2), 40.3 (CH_2), 79.2 (O–C), 156.1 (CO), 178.9 (CO) ppm; elemental analysis calcd (%) for $C_{11}H_{21}NO_4$ (231.3): C 57.12, H 9.15, N 6.06; found: C 56.84, H 9.26, N 6.21; MS (ESI): *m/z*: 254 $[M+Na]^+$.

Ethyl 1-methyl-4-[1-methyl-4-[(5-*tert*-butyloxycarbonylaminopentyl)-carboxamido]pyrrole-2-carboxamido]pyrrole-2-carboxylate (15): A suspension of nitro compound **11**[35] (2.08 g, 6.5 mmol) in MeOH (600 mL) was hydrogenated for 5 h at room temperature under a 5-bar pressure in the presence of 5% Pd on activated charcoal (1 g). The catalyst was then removed by filtration, and the MeOH eliminated under reduced pressure. Acid **14** (1.70 g, 7.36 mmol) and EDC (1.41 g, 7.37 mmol) were added to the solution of the resulting oily amine **12** (1.77 g, 94%) in DMF (30 mL). The reaction mixture was stirred at room temperature for 24 h, and the DMF was then removed under reduced pressure. The resulting oil was purified by chromatography (ligroin/EtOAc, 50:50 to 0:100). Compound **15** was purified by dissolution in EtOAc and precipitation by addition of cyclohexane to give a white solid (2.15 g, 70%). M.p.: 148–150 °C; IR (KBr): $\tilde{\nu}$ = 3353, 3309, 3250, 1716, 1702, 1685 cm^{-1}; ^1H NMR ([D$_6$]DMSO): δ = 1.29 (5H, m; CH_2CH_3, CH_2), 1.38 (11H, m; $C(CH_3)_3$, CH_2), 1.57 (2H, m; CH_2), 2.23 (2H, t; CH_2CO), 2.90 (2H, m; $NHCH_2$), 3.83 (3H, s; NCH_3), 3.85 (3H, s; NCH_3), 4.21 (2H, q; CH_2CH_3), 6.80 (1H, t; $NHCH_2$), 6.90, 6.93, 7.19, 7.45 (4H, 4s; 4 pyrrolic H), 9.78 (1H, s; NH), 9.90 (1H, s; NH) ppm; ^{13}C NMR ([D$_6$]DMSO): δ = 15.3 (CH_3), 26.1 (CH_2), 27.1 (CH_2), 29.3 (3CH_3), 30.4 (CH_2), 36.7 (CH_2), 37.0 (NCH_3), 37.1 (NCH_3), 39.8 (CH_2), 60.4 (OCH_2), 78.3 (O–C), 105.1 (CH), 109.5 (CH), 119.3 (CH), 119.9 (Cq), 121.6 (CH), 123.2 (Cq), 123.5 (Cq), 123.9 (Cq), 156.6 (CO), 159.4 (CO), 161.4 (CO), 170.5 (CO) ppm; elemental analysis calcd (%) for $C_{25}H_{37}N_5O_6$ (503.6): C 59.63, H 7.41, N 13.91; found: C 59.51, H 7.34, N 13.88; MS (ESI): *m/z*: 526 $[M+Na]^+$.

1-Methyl-4-[1-methyl-4-[(5-*tert*-butyloxycarbonylaminopentyl)-carboxamido]pyrrole-2-carboxamido]pyrrole-2-carboxylic acid (16): A solution of NaOH (0.68 g, 17 mmol) in water (30 mL) was added to a solution of ester **15** (1.72 g, 3.42 mmol) in MeOH (20 mL). The mixture was heated at 60 °C for 3 h, cooled, and then acidified to pH 2 with 6 M HCl. After addition of water and stirring overnight, the precipitate was filtered off, washed with water, and dried to give **16** as a white solid (1.46 g, 90%). M.p.: 180–182 °C; IR (KBr): $\tilde{\nu}$ = 3587, 3392, 3284, 1691, 1689 cm^{-1}; ^1H NMR ([D$_6$]DMSO): δ = 1.28 (2H, m; CH_2), 1.40 (11H, m; $C(CH_3)_3$, CH_2), 1.58 (2H, m; CH_2), 2.24 (2H, t; CH_2CO), 2.91 (2H, m; CH_2NH), 3.84 (6H, s; 2NCH_3), 6.86 (3H, m; 2 pyrrolic H, $NHCH_2$), 7.17, 7.45 (2H, 2s; 2 pyrrolic H), 9.80 (1H, s; NH), 9.90 (1H, s; NH), 10.61 (1H, s; COOH) ppm; ^{13}C NMR ([D$_6$]DMSO): δ = 26.2 (CH_2), 27.1 (CH_2), 29.3 (3CH_3), 30.4 (CH_2), 36.7 (CH_2), 37.0 (NCH_3), 37.1 (NCH_3), 39.8 (CH_2), 78.3 (OC), 105.1 (CH), 109.5 (CH), 119.2 (CH), 120.6 (Cq), 121.3 (CH), 123.2 (Cq), 123.7 (2Cq), 156.6 (CO), 159.5 (CO), 163.0 (CO), 170.5 (CO) ppm; elemental analysis calcd (%) for $C_{23}H_{33}N_5O_6$ (475.5): C 58.09, H 6.99, N 14.73; found: C 57.69, H 6.91, N 14.36; MS (ESI): *m/z*: 498 $[M+Na]^+$.

4-(9-Acridinylamino)-*N*-[4-[[4-[[(5-*tert*-butyloxycarbonylamino)-pentyl]carbonylamino]-1-methylpyrrole-2-yl]carbonylamino]-1-methylpyrrole-2-carbonyl]glycylaniline (17): A solution of acid **16** (1.26 g, 2.65 mmol), EDC (924 mg, 4.82 mmol), HOBt (651 mg, 4.82 mmol), acridine **6** (1 g, 2.41 mmol), and Et_3N (1.10 mL, 7.91 mmol) in DMF (50 mL) was stirred at room temperature for 24 h. After removal of the DMF under reduced pressure, the resulting oil was dissolved in MeOH. Addition of Et_2O afforded a precipitate that was purified by flash chromatography (dichloromethane/MeOH, 95:5 to 85:15) to give **17** as an orange solid (1.31 g, 62%). M.p.: 227–228 °C; IR (KBr): $\tilde{\nu}$ = 3274, 1682, 1636 cm^{-1}; ^1H NMR ([D$_6$]DMSO): δ = 1.30 (2H, m; CH_2), 1.41 (11H, m; $C(CH_3)_3$, CH_2), 1.59 (2H, m; CH_2), 2.27 (2H, t; CH_2CO), 2.92 (2H, m; $NHCH_2$), 3.84 (6H, s; 2NCH_3), 4.05 (2H, d; $NHCH_2CO$), 6.83 (1H, t; $NHCH_2$), 6.92, 7.00, 7.18, 7.28 (4H, 4s; 4 pyrrolic H), 7.42 (4H, m; arH), 7.81 (2H, m; arH), 8.01 (4H, m; arH), 8.25 (2H, m; arH), 8.43 (1H, t; $NHCH_2$), 9.80 (1H, s; NH), 9.97 (1H, s; NH), 10.40 (1H, s; NH), 11.40 (1H, s, NH) ppm; ^{13}C NMR ([D$_6$]DMSO): δ = 26.2 (CH_2), 27.1 (CH_2), 29.3 (3CH_3), 30.4 (CH_2), 36.6 (CH_2), 37.1 (2NCH_3), 40.1 (CH_2), 43.9 (CH_2), 78.4 (O–C), 105.2 (CH), 105.8 (CH), 114.8 (2Cq), 119.2 (CH), 119.4 (CH), 120.1 (2CH), 121.1 (2CH), 123.1 (Cq), 123.3 (2Cq), 123.7 (Cq), 124.4 (2CH), 125.9 (2CH), 126.8 (2CH), 135.8 (2CH), 137.4 (Cq), 139.2 (Cq), 141.2 (2Cq), 155.8 (Cq), 156.6 (CO), 159.5 (CO), 162.7 (CO), 169.1 (CO), 170.6 (CO) ppm; elemental analysis calcd (%) for $C_{44}H_{49}N_9O_6$ (799.9): C 66.07, H 6.17, N 15.76; found: C 65.81, H 6.34, N 15.52; MS (ESI): *m/z*: 800 $[MH]^+$.

4-(9-Acridinylamino)-*N*-[4-[[4-[(5-aminopentyl)carbonylamino]-1-methylpyrrole-2-yl]carbonylamino]-1-methylpyrrole-2-carbonyl]-glycylaniline trifluoroacetate (18): A suspension of derivative **17** 520 mg, 0.65 mmol) in TFA (26 mL) was stirred at 0 °C for 35 min. After removal of TFA, the residue was triturated with Et_2O. The resulting precipitate was filtered off and washed with Et_2O to afford an orange powder (525 mg, 100%). M.p.: 198–199 °C; IR (KBr): $\tilde{\nu}$ = 3266, 3095, 1678 cm^{-1}; ^1H NMR ([D$_6$]DMSO): δ = 1.36 (2H, m; CH_2), 1.58 (4H, m; 2CH_2), 2.26 (2H, t; CH_2CO), 2.79 (2H, m; $CH_2{-}^+NH_3$), 3.84 (6H, s; 2NCH_3), 4.02 (2H, d; $NHCH_2CO$), 6.89, 7.00, 7.17, 7.25 (4H, 4s; 4 pyrrolic H), 7.47 (4H, m; arH), 7.66 (3H, br s; NH_3), 7.80 (2H, m; arH), 8.00 (4H, m; arH), 8.22 (2H, m; arH), 8.39 (1H, t; $NHCH_2$), 9.81 (1H, s; NH), 9.92 (1H, s; NH), 10.24 (1H, s; NH), 11.45 (1H, s; NH) ppm; ^{13}C NMR ([D$_6$]DMSO): δ = 25.9 (CH_2), 26.6 (CH_2), 27.9 (CH_2), 36.6 (CH_2), 37.1 (2NCH_3), 39.8 (CH_2), 43.9 (CH_2), 105.1 (CH), 105.8 (CH), 114.8 (2Cq), 119.2 (CH), 119.4 (CH), 120.2 (2CH), 121.2 (2CH), 123.1 (Cq), 123.3 (2Cq), 123.8 (Cq), 124.5 (2CH), 125.9 (2CH), 126.7 (2CH), 136.1 (2CH), 137.4 (Cq), 139.2 (Cq), 141.2 (2Cq), 155.9 (Cq), 159.5 (CO), 162.7 (CO), 169.5 (CO), 170.4 (CO) ppm; MS (ESI): *m/z*: 700 $[M-CF_3CO_2]^+$.

R-132: A solution of phenanthridinium acid **10** (154 mg, 0.338 mmol), EDC (130 mg, 0.676 mmol), HOBt (91 mg, 0.676 mmol), amine **18** (314 mg, 0.338 mmol), and Et_3N (0.141 mL, 1.015 mmol) was stirred at room temperature for 20 h. After addition of Et_2O, the precipitate was filtered off. **R132** was purified by flash chromatography (dichloromethane/MeOH/1 M HCl in MeOH, 90:10:0 to 75:25:0.1) to give **R-132** as a red solid (120 mg, 32%). M.p.: 302–304 °C (decomp.); IR (KBr): $\tilde{\nu}$ = 3334, 1644 (broad bands) cm^{-1}; ^1H NMR ([D$_6$]DMSO): δ = 1.40 (5H, m; NCH_2CH_3, CH_2), 1.65 (4H, m; 2CH_2), 2.30 (2H, t; CH_2CO), 3.40 (2H, m; $NHCH_2$), 3.81 (3H, s; NCH_3), 3.82 (3H, s; NCH_3), 4.05 (2H, m; $NHCH_2CO$), 4.46 (2H, m; $^+NCH_2CH_3$), 6.00 (2H, br s; NH_2), 6.25 (1H, m; arH), 6.45 (2H, br s; NH_2), 6.92, 6.98, 7.20, 7.26 (4H, 4s; 4arH), 7.45 (7H, m; arH), 7.81 (4H, m; arH), 8.00 (2H, m; arH), 8.10 (2H, m; arH), 8.25 (4H, m; arH), 8.42 (1H, t; $NHCH_2$), 8.65 (2H, m; arH), 8.90 (1H, t; $NHCH_2$), 9.90 (1H, s; NH), 10.00 (1H, s; NH), 10.50 (1H, s; NH), 11.60 (1H, s, NH), 11.90 (1H, s, NH) ppm; ^{13}C NMR ([D$_6$]DMSO): δ = 14.7 (CH_3), 26.2 (CH_2), 27.3 (CH_2), 30.0 (CH_2), 36.6 (CH_2), 37.1 (2NCH_3), 40.3 (CH_2), 43.9 (CH_2), 50.2 (NCH_2), 99.3 (CH), 105.2 (CH), 105.8 (CH), 108.7 (CH), 114.7 (2Cq), 118.5 (Cq), 119.2 (CH), 119.4 (CH), 120.2 (2CH), 121.3 (3CH), 123.1 (Cq), 123.3 (Cq), 123.4 (Cq), 123.6 (Cq), 123.7 (CH), 124.5 (2CH), 125.7 (2CH), 125.9 (Cq), 126.1 (2CH), 126.8 (2CH), 128.5 (Cq), 129.0 (CH),129.1 (2CH), 129.6 (2CH), 135.2 (Cq), 135.6 (Cq), 136.0 (2CH), 137.3 (Cq), 137.4 (Cq), 139.4 (Cq), 141.2 (2Cq), 149.1 (Cq), 152.2 (Cq), 156.0 (Cq), 158.8 (Cq), 159.5 (CO), 162.6 (CO), 166.1 (CO), 169.6 (CO), 170.6 (CO) ppm; HRMS: *m/z* calcd for $[M-2Cl]^{2+}$: 520.2405; found: 520.2382.

Chemicals and biochemicals: Calf thymus DNA and the double-stranded polymers poly(dAT)$_2$ and poly(dGC)$_2$ were purchased from Sigma Chemical Co. (La Verpillière, France). Calf thymus DNA was deproteinized with SDS. All other chemicals were analytical grade reagents.

Absorption spectra and melting temperature studies: Melting curves were measured with an Uvikon 943 spectrophotometer coupled to a Neslab RTE111 cryostat. For each series of measurements, 12 samples were placed in a thermostatically controlled cell-holder, and the quartz cuvettes (10 mm pathlength) were heated by

circulating water. Measurements were performed in BPE buffer (6 mM Na_2HPO_4, 2 mM NaH_2PO_4, 1 mM ethylenediaminetetraacetate (EDTA); pH 7.0). The temperature inside the cuvette was measured with a platinum probe; it was increased over the range 20 – 100 °C with a heating rate of 1 °C min^{-1}. The "melting temperature" (T_m) was taken as the midpoint of the hyperchromic transition. The Uvikon 943 spectrophotometer was also used to record the absorption spectra.

Determination of binding constants by surface plasmon resonance (SPR): The 5′-biotin-substituted hairpin DNA oligonucleotide used for the SPR studies (5′-biotin-dCGAATTCGTCTCCGAATTCG-3′, hairpin loop underlined) was obtained as an HPLC-purified product from Eurogentec. Ethidium bromide (Aldrich) is readily soluble in water. A stock solution (80 μM) of the drug **R-132** was prepared in water. Surface plasmon resonance (SPR) measurements were performed with a four-channel BIAcore 3000 optical biosensor system and streptavidin-coated sensor chips (SA). To prepare the sensor chips for use, they were conditioned with several consecutive 1-min injections of 1 M NaCl in 50 mM NaOH followed by two 1-min injections of 0.1 % SDS in 3.5 mM EDTA and extensive washing with HBS-EP buffer (0.01 M 2-[4-(2-hydroxyethyl)-1-piperazinyl]ethanesulfonic acid, pH 7.4, 0.15 M NaCl, 3 mM EDTA, 0.0005 % Surfactant P20, sterile filtered and degassed buffer obtained from Biacore). Nearly the same amounts of 5′-biotinylated oligomers (25 nM) in HBS-EP buffer were immobilized on the surface by noncovalent capture with one of the flow cells left blank as a control. Manual injection was used with a flow rate of 2 μL min^{-1} to achieve long contact times with the surface and to control the amount of DNA bound to the surface. Solutions of compound with known concentrations were prepared in filtered and degassed buffer by serial dilutions from stock solution and passed over the immobilized DNA surfaces for a predetermined time period (typically 10 – 20 min) at a flow rate of 30 μL min^{-1} and at 25 °C. Buffer flow alone over 20 min was sufficient to dissociate the drug from the DNA for surface regeneration.

Average fitting of the sensorgrams at the steady-state level was performed with the BIAevaluation 3.0 program. To obtain the affinity constants, the results from the steady-state region were fitted with a one-site interaction model by using Kaleidagraph for nonlinear least squares optimization of the binding parameters from the following equation:

$$r = (nK_{eq} \times C_{free})/(1 + K_{eq} \times C_{free})$$

where r represents the moles of bound compound per mole of DNA hairpin duplex, K_{eq} is the macroscopic binding constant, C_{free} is the compound concentration in equilibrium with the complex fixed by the concentration in the flow solution, and n is the number of compound binding sites on the DNA duplex. The r values are calculated from the ratio RU/RU_{max} where RU is the steady-state response at each concentration and RU_{max} is the predicted RU value for binding of a single compound to the DNA on a flow cell. The RU_{max} value is determined from the DNA molecular weight, amount of DNA on the flow cell, the compound molecular weight, and the refractive index gradient ratio of the compound and DNA.[38] The K values are determined for each set of sensorgrams by nonlinear least square fitting of r versus C_{free} plots for compound bound to each DNA.

Circular dichroism: CD spectra were recorded on a Jobin – Yvon CD6 dichrograph interfaced to a microcomputer. Solutions of drugs, nucleic acids, and their complexes (3 mL in 1 mM sodium cacodylate buffer, pH 7.0) were scanned in 2-cm quartz cuvettes. Measurements were made by progressive dilution of drug – DNA complex at a high P/D (phosphate/drug) ratio with a pure ligand solution to yield the desired drug/DNA ratio. Four scans were accumulated and automatically averaged.

Electric linear dichroism measurements (ELD): ELD measurements were performed with a computerized optical measurement system by the procedures previously outlined.[39] All experiments were conducted with a 10-mm-pathlength Kerr cell with a 1.5-mm electrode separation. The samples were oriented under an electric field strength varying from 1 to 14 kV cm^{-1}. The drug was present at 10 μM concentration together with the DNA or polynucleotide at 200 μM concentration unless otherwise stated. This electro-optical method has proved most useful to determine the orientation of the drugs bound to DNA. It has the additional advantage that it senses only the orientation of the polymer-bound ligand. Free ligand is isotropic and does not contribute to the signal.[40]

DNase I footprinting: The 176-bp DNA fragment was prepared by 3′-[^{32}P]-end labeling of the *Eco*RI – *Pvu*II double digest of the plasmid pTUC with α-[^{32}P]-dATP (3000 Ci mmol^{-1}, Amersham, Buckinghamshire, England) and AMV reverse transcriptase. DNase I footprinting experiments were performed essentially as previously described.[41] Briefly, samples (3 μL) of the labeled DNA fragment were incubated with the buffered solution (5 μL) containing the ligand at appropriate concentration. After 30 min incubation at 37 °C to ensure equilibration of the binding reaction, the digestion was initiated by the addition of a DNase I (2 μL, 0.01 unit mL^{-1}). After 3 min, the reaction was stopped by freeze-drying. Samples were lyophilized and resuspended in an 80 % formamide solution (5 μL) containing tracking dyes. The DNA samples were then heated at 90 °C for 4 min and chilled in ice for 4 min prior to electrophoresis.

Topoisomerase-mediated DNA relaxation: Supercoiled pKMp27 DNA (0.5 μg) was incubated with 4 units human topoisomerase I or II (TopoGen) at 37 °C for 1 h in relaxation buffer (50 mM tris(hydroxymethyl)aminomethane (pH 7.8), 50 mM KCl, 10 mM $MgCl_2$, 1 mM dithiothreitol, 1 mM EDTA and ATP) in the presence of varying concentrations of the test compounds. Reactions were terminated by addition of SDS to 0.25 % and proteinase K to 250 μg mL^{-1}. DNA samples were then added to the electrophoresis dye mixture (3 μL) and were electrophoresed in a 1 % agarose gel containing ethidium bromide (1 μg mL^{-1}) at room temperature for 2 h at 120 V. Gels were washed and photographed under UV light.

Cell cultures and survival assay: Murine P388 murine leukemia cells were grown at 37 °C in a humidified atmosphere containing 5 % CO_2 in RPMI 1640 medium, supplemented with 10 % fetal bovine serum, glutamine (2 mM), penicillin (100 IU mL^{-1}) and streptomycin (100 μg mL^{-1}). The cytotoxicity of the drug was assessed by using a cell proliferation assay developed by Promega (CellTiter 96 Aqueous One Solution Cell Proliferation Assay). Briefly, 2×10^4 exponentially growing cells were seeded in 96-well microculture plates with various drug concentrations in a volume of 100 μL. After 72 h incubation at 37 °C, the aqueous soluble tetrazolium dye (20 μL of MTS[42]) was added to each well and the samples were incubated for a further 3 h at 37 °C. Plates were analyzed on a Labsystems Multiskan MS (type 352) reader at 492 nm.

Fluorescence microscopy: The cells (20 000 cells cm^{-2}) were incubated at 37 °C with **R-132** (10 μM) for 18 h. The medium was removed and cells were rinsed with ice-cold phosphate-buffered saline for 10 min prior to fixation with a 2 % paraformaldehyde solution for 20 min at 4 °C. A drop of antifade solution was added and the treated portion of the slide was covered with a glass coverslip. The fluorescence of the drug was detected and localized by confocal microscopy with a Leica DMIRBE microscope controlled by a Leica

TCS-NT workstation (Leica Microsystems, Bensheim, Germany) with a 63 × 1.32 NA oil objective, equipped with a 75 mW argon-krypton laser line.

This work was done with the support from research grants to C.B. from the Ligue Nationale Contre le Cancer (Equipe labellisée LA LIGUE); to C.H. and P.C. from the Actions de Recherches Concertées, Contract no. 95/00 – 93. This research was supported by a Marie Curie Fellowship of the European Community Programme "Improving Human Research Potential and the Socio-Economic Knowledge Base" under contract no. HPMFCT-2000 – 00701 (to C.C.). We thank the Service Commun d'Imagerie Cellulaire de l'IFR22 for access to the confocal microscope and the BIAcore 3000 instrumentation. Support by the "Actions intégrées Franco-Belges, Programme Tournesol" is acknowledged. M.H. thanks the National Council for Scientific Research of Lebanon for financial support. Nathalie Cholleton and Estelle Payant are acknowledged for technical chemical assistance.

[1] C. Bailly, in *Advances in DNA Sequence Specific Agents*, *Vol. 3* (Ed.: M. Palumbo), JAI Press, **1998**, pp. 97 – 156.
[2] D. E. Thurston, *Br. J. Cancer* **1999**, *80*, 65 – 85.
[3] C. Bailly, N. Pommery, R. Houssin, J. P. Hénichart, *J. Pharm. Sci.* **1989**, *78*, 910 – 917.
[4] C. Bailly, J. B. Chaires, *Bioconjugate Chem.* **1998**, *9*, 513 – 538.
[5] C. Bailly, J. P. Hénichart, *Bioconjugate Chem.* **1991**, *2*, 379 – 393.
[6] C. Bailly, J. P. Hénichart, in *Molecular Aspects of Anticancer Drug – DNA Interactions*, *Vol. 2* (Eds.: S. Neidle, M. J. Waring), Macmillan, London, **1994**, pp. 162 – 196.
[7] C. Bailly, M. Collyn-d'Hooghe, D. Lantoine, C. Fournier, B. Hecquet, P. Fosse, J. M. Saucier, P. Colson, C. Houssier, J. P. Hénichart, *Biochem. Pharmacol.* **1992**, *43*, 457 – 466.
[8] C. Bailly, C. OhUigin, R. Houssin, P. Colson, C. Houssier, C. Rivalle, E. Bisagni, J. P. Hénichart, M. J. Waring, *Mol. Pharmacol.* **1992**, *41*, 845 – 855.
[9] C. Bailly, J. S. Sun, P. Colson, C. Houssier, C. Hélène, M. J. Waring, J. P. Hénichart, *Bioconjugate Chem.* **1992**, *3*, 100 – 103.
[10] C. Bourdouxhe, P. Colson, C. Houssier, J. S. Sun, T. Montenay-Garestier, C. Hélène, C. Rivalle, E. Bisagni, M. J. Waring, J. P. Hénichart, C. Bailly, *Biochemistry* **1992**, *31*, 12 385 – 12 396.
[11] G. Anneheim-Herbelin, M. Perrée-Fauvet, A. Gaudemer, P. Helissey, S. Giorgi-Renault, *Tetrahedron Lett.* **1993**, *34*, 7263 – 7266.
[12] C. Bailly, V. Leclère, N. Pommery, P. Colson, C. Houssier, C. Rivalle, E. Bisagni, J. P. Hénichart, *Anti-Cancer Drug Des.* **1993**, *8*, 145 – 164.
[13] C. Bailly, C. Michaux, P. Colson, C. Houssier, J. S. Sun, T. Garestier, C. Hélène, J. P. Hénichart, C. Rivalle, E. Bisagni, M. J. Waring, *Biochemistry* **1994**, *33*, 15 348 – 15 364.
[14] P. Fossé, B. René, J. M. Saucier, J. P. Hénichart, M. J. Waring, P. Colson, C. Houssier, C. Bailly, *Biochemistry* **1994**, *33*, 9865 – 9874.
[15] P. Herfeld, P. Helissey, S. Giorgi-Renault, *Bioconjugate Chem.* **1994**, *5*, 67 – 76.
[16] B. Plouvier, R. Houssin, B. Hecquet, P. Colson, C. Houssier, M. J. Waring, J. P. Hénichart, C. Bailly, *Bioconjugate Chem.* **1994**, *5*, 475 – 481.
[17] K. E. Rao, G. Gosselin, D. Mrani, C. Périgaud, J. L. Imbach, C. Bailly, J. P. Hénichart, P. Colson, C. Houssier, J. W. Lown, *Anti-Cancer Drug Des.* **1994**, *9*, 221 – 237.
[18] M. Bouziane, C. Ketterlé, P. Helissey, P. Herfeld, M. Le Bret, S. Giorgi-Renault, C. Auclair, *Biochemistry* **1995**, *34*, 14 051 – 14 058.
[19] A. W. McCaunaughie, T. C. Jenkins, *J. Med. Chem.* **1995**, *38*, 3488 – 3501.
[20] C. Bourdouxhe-Housiaux, P. Colson, C. Houssier, M. J. Waring, C. Bailly, *Biochemistry* **1996**, *35*, 4251 – 4264.
[21] P. Hélissey, C. Bailly, J. N. Vishwakarma, C. Auclair, M. J. Waring, S. Giorgi-Renault, *Anti-Cancer Drug Des.* **1966**, *11*, 527 – 551.
[22] C. Ketterlé, J. Gabarro-Arpa, M. Ouali, M. Bouziane, C. Auclair, P. Helissey, S. Giorgi-Renault, M. Le Bret, *J. Biomol. Struct. Dyn.* **1996**, *13*, 963 – 973.
[23] N. Boitte, N. Pommery, P. Colson, C. Houssier, M. J. Waring, J. P. Hénichart, C. Bailly, *Anti-Cancer Drug Des.* **1997**, *12*, 481 – 501.
[24] J. P. Hénichart, M. J. Waring, J. F. Riou, W. A. Denny, C. Bailly, *Mol. Pharmacol.* **1997**, *51*, 448 – 461.
[25] P. Herfeld, P. Hélissey, J. Nafziger, S. Giorgi-Renault, *Anti-Cancer Drug Des.* **1998**, *13*, 337 – 359.
[26] P. Helissey, S. Giorgi-Renault, P. Colson, C. Houssier, C. Bailly, *Bioconjugate Chem.* **2000**, *11*, 219 – 227.
[27] C. Bailly, N. Helbecque, J. P. Hénichart, P. Colson, C. Houssier, K. E. Rao, R. G. Shea, J. W. Lown, *J. Mol. Recognit.* **1990**, *3*, 26 – 35.
[28] C. Bailly, J. P. Hénichart, *Biochem. Biophys. Res. Commun.* **1990**, *167*, 798 – 806.
[29] M. Waring, in *Antibiotics*, *Vol. III* (Eds.: J. W. Corcoran, F. E. Hahn), Springer, New York, **1975**, pp. 141 – 165.
[30] J. P. Hénichart, J. L. Bernier, J. P. Catteau, *Hoppe-Seyler's Z. Physiol. Chem.* **1982**, *363*, 835 – 841.
[31] P. B. Dervan, M. M. Becker, *J. Am. Chem. Soc.* **1978**, *100*, 1968 – 1970.
[32] P. B. Dervan, R. P. Hertzberg, US Patent 4665184, **1987**; [*Chem. Abstr.* **1987**, *107*, P232672b].
[33] R. L. Letsinger, M. E. Schott, *J. Am. Chem. Soc.* **1981**, *103*, 7394 – 7396.
[34] T. Konakahara, R. L. Wurdeman, B. Gold, *Biochemistry* **1988**, *27*, 8606 – 8613.
[35] R. Fishleigh, K. Fox, A. Khalaf, A. Pitt, M. Scobie, C. Suckling, J. Urwin, R. Waigh, S. Young, *J. Med. Chem.* **2000**, *43*, 3257 – 3266.
[36] C. Bailly, *Methods Enzymol.* **2001**, *340*, 610 – 623.
[37] V. Guelev, J. Lee, J. Ward, S. Sorey, D. W. Hoffman, B. L. Iverson, *Chem. Biol.* **2001**, *8*, 415 – 425.
[38] T. M. Davis, W. D. Wilson, *Anal. Biochem.* **2000**, *284*, 348 – 353.
[39] C. Houssier, in *Molecular Electro-Optics* (Ed.: S. Krause), Plenum, New York, **1981**, pp. 363 – 398.
[40] P. Colson, C. Bailly, C. Houssier, *Biophys. Chem.* **1996**, *58*, 125 – 140.
[41] C. Bailly, M. J. Waring, *J. Biomol. Struct. Dyn.* **1995**, *12*, 869 – 898.
[42] A. H. Cory, T. C. Owen, J. A. Barltrop, J. G. Cory, *Cancer Commun.* **1991**, *3*, 207 – 212.

Received: July 8, 2002 [F 452]